View metadata, citation and similar papers at core.ac.uk

brought to you by CORE

provided by Tomsk State University Repository

Stress-Induced Thermoelastic Martensitic Transformations and Functional Properties in [011]-oriented NiTiHfPd Single Crystals

This content has been downloaded from IOPscience. Please scroll down to see the full text.

2015 IOP Conf. Ser.: Mater. Sci. Eng. 93 012048

(http://iopscience.iop.org/1757-899X/93/1/012048)

View the table of contents for this issue, or go to the journal homepage for more

Download details:

IP Address: 92.63.68.149
This content was downloaded on 22/10/2015 at 04:09

Please note that terms and conditions apply.

Stress-Induced Thermoelastic Martensitic Transformations and Functional Properties in [011]-oriented NiTiHfPd Single Crystals

A I Tagiltsev[1], E E Timofeeva[1], E Yu Panchenko[1] and Yu I Chumlyakov[1]

[1] Tomsk State University, Siberian Physical-Technical Institute, Tomsk, 634050, Russia

E-mail: antontgl@gmail.com, katie@sibmail.com, panchenko@mail.tsu.ru, chum@phys.tsu.ru, karaca@engr.uky.edu

Abstract. The stress-induced martensitic transformation in the [011]-oriented $Ni_{45.3}Ti_{29.7}Hf_{20}Pd_5$ (at. %) single crystals in as-grown, homogenized and aged states were investigated in compression. It is experimentally shown that heat treatments of single crystals result in increase in martensitic transformation temperatures, two-fold decrease in reversible strain and increase in strain-hardening coefficient. As-grown single crystals demonstrate large temperature range of superelasticity (up to 140 K), large reversible strain (up to 4.3 %) and large work output in comparison with homogenized and aged crystals.

1. Introduction

Alloys with thermoelastic martensitic transformations (MT) are used in wide range of applications. A shape memory effect (SME) and superelasticity (SE) are observed due to the thermoelastic nature of transformation. TiNi is one of mostly usable materials with MT [1]. However, it is known [2] that TiNi alloys demonstrate low transformation and work temperatures (<373 K) and low strength (<700 MPa) that limit its application. Hf and Pd are used as alloying elements to exclude these problems. NiTiHf and NiTiHfPd alloys have high strength properties (critical stress level of stress-induced MT ~1000 MPa) and high damping ability owing to wide mechanical hysteresis (~400 MPa) and promising potential for high damping and high strength applications [3].

It is known that, the control of functionality and mechanical properties of the alloys is possible due to heat treatments. The functional behavior of NiTi alloys can be improved by heat treatments, it is natural to extend such studies to determine the effects of precipitate strengthening on shape memory and functional properties [3]. The aging results in variations of the degree order of high-temperature phase, precipitation of the second-phase particles, which causes changes in MT temperatures, transformation strain, critical stress for stress-induced MT, hardening of the matrix change and so on [2, 4-6]. On these reasons this work is aimed to investigate the effects of heat treatment on stress-induced MT and functional properties in compression in [011]-oriented $Ni_{45.3}Ti_{29.7}Hf_{20}Pd_5$ (at. %) single crystals after different heat treatments.

2. Materials and methods

Content from this work may be used under the terms of the Creative Commons Attribution 3.0 licence. Any further distribution of this work must maintain attribution to the author(s) and the title of the work, journal citation and DOI.
Published under licence by IOP Publishing Ltd

The single crystals were grown using the Bridgeman method in an inert gas atmosphere. Samples (3 mm x 3 mm x 6 mm) were electro-discharge machined, then mechanically and electrolitically polished in electrolyte 5% $HClO_4$ + 95% CH_3COOH under T=293 K, U=20 B. The sample orientation was verified with DRON-3 X-ray diffractometer. Orientation [011] was chosen due to the highest value of transformation strain that is confirmed by theoretical calculations [7].

The single crystals were investigated in following conditions: as-grown without any additional heat treatments (type-I), homogenized at 1323 K for 4 h (type-II), homogenized at 1323 K for 4 h followed by ageing at 1173 K for 3 h and water quenching (type-III). The homogenization was carried out in quartz tubes in an inert gas atmosphere followed by slow cooling of crystals (cooling rate is about 20-30 $K \cdot min^{-1}$).

The experiments of cooling/heating under constant stresses in range from 0 to 300 MPa (ε(T) response) and the experiments of loading/unloading at isothermal conditions in range from 300 to 473 K (σ(ε) response) were carried out for investigation the stress-induced MT.

Mechanical experiments in compression were conducted on following installations: Instron testing machine 5969; miniature load frame for measuring reversible strain under the constant stress level during cooling/heating. The analysis of single crystal surface was performed by optical microscopy using the universal measuring complex Keyence VHX-2000. Transmission electron microscopy (TEM) was accomplished using electron microscope JEM-2010. Semiquantitative elemental analysis was carried out on scanning electron microscope Supra VP55. Distribution of chemical elements (Ti, Ni, Hf, Pd) was obtained by JEOL 8900 Electron Probe Microanalyzer.

3. Results and discussion

It was observed that as-grown single crystals contain dendrites (figure 1) that is also shown in [7]. Dendrites volume fraction is about 8-9%. The homogenization didn't result in complete dissolution of dendrites (figure 1) but leads to three-fold decrease of dendrites volume fraction. Chemical elements (Ti, Ni, Hf, Pd) distribution was investigated: all elements uniformly allocated both in matrix and in dendrites. Dendrites are richer in Hf (84.6 at.%), poorer in Ti (15.3 at.%) and contain almost no Ni and Pd (0 and 0.1 at. %). The chemical composition of the matrix was defined as Ni = 46.4 at.%, Ti = 30.7 at.%, Hf = 18.3 at.%, Pd = 4.6 at.% that is very close to the nominal composition within 5 % error. It is shown (figure 1(b)), that high-temperature phase of all investigated single crystals has B2 structure. As presented in [8], NiTiHfPd single crystals transform to monoclinic B19' martensite.

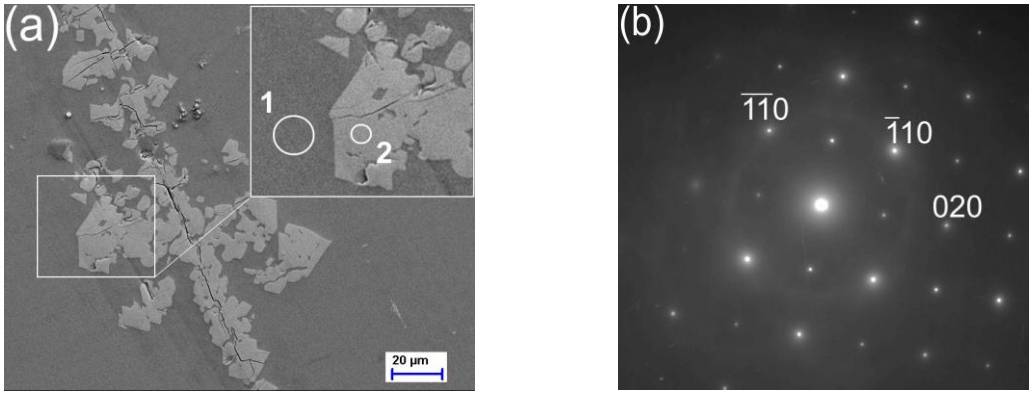

Figure 1. The type-II NiTiHfPd single crystals surface. Numbers indicate the areas where semiquantitative elemental analysis was carried out: 1 – matrix, 2 – dendrite (a); selected-area diffraction pattern of austenite phase exhibiting B2-structure in type-I NiTiHfPd single crystals, zone axis $[001]_{B2}$ (b).

Figure 2 demonstrates ε(T) response for all investigated crystals I-III, received at cooling/heating under the constant stress level. Minimal stress level necessary to destruct the self-accomodation system and to form the oriented martensite at cooling/heating under the constant stress level is

50 MPa. The reversible strain at 50 MPa is about 0.5 % in all investigated crystals. Martensite oriented relative to external stress axis, is going to grow at cooling below T= $M_{s'}$. After $M_{f'}$ the forward transformation is over. At T = $A_{s'}$ the reverse transformation begins. It should be noted, that given strain is reversible at T > $A_{f'}$ and SME is observed. As marked for the ε(T) response in figure 2 transformation strain ε_{rev} and thermal hysteresis ΔT were defined as the horizontal and vertical width of the loops, respectively. The value of reversible strain increases with increase in external stress levels in all studied states I-III (figure 3).

Maximal reversible strain in type-I single crystals is obtained under 250 MPa and equals 4.3 %. This value doesn't change at further increase of applied stress level. It is shown [2, 3, 9, 10], that maximal reversible strain doesn't exceed 4.5 % in different states of NiTiHfPd alloys (homogenization at 1173 K for 72 h, homogenization at 1323 K followed by ageing at 973 K for 72 h, homogenization at 1323 K followed by ageing at 923 K for 3 h).

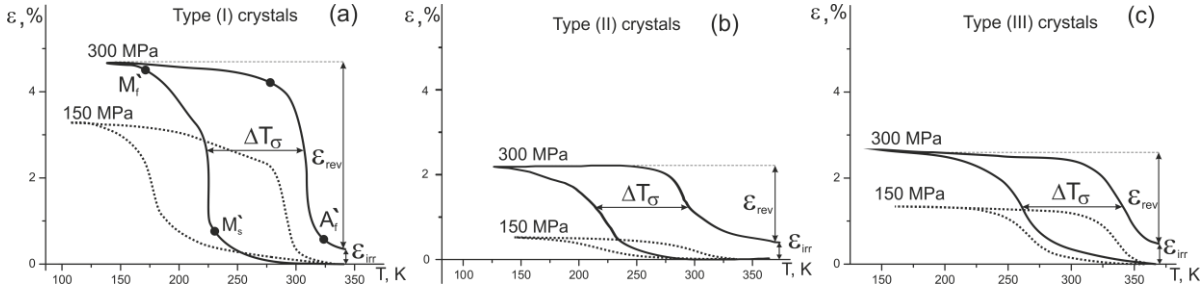

Figure 2. The ε(T) response for type-I (a), type-II (b), type-III (c) NiTiHfPd single crystals.

In type-II and type-III single crystals the reversible strain slowly increases with increase of stresses and saturation such in type-I crystals is not observed. However, the appearance of irreversible strain under 250-300 MPa is indirect evidence of reaching maximal reversible strain values. Reversible strains decrease to 1.7 % and 2 % in type-II and type-III crystals, respectively, in comparison with type-I crystals. The irreversible strain doesn't exceed 0.4% in all investigated crystals.

Work output is an important property of shape memory materials in the design of functional devices such as solid state actuators [3]. In this case, work output can be calculated by multiplying the applied stress by the corresponding reversible strain from the experiments of cooling/heating under constant stresses [3, 11]. Figure 3 shows the work output values as a function of applied stress for all investigated single crystals. Work output increases with applied stress. Type-I single crystals demonstrate the reversible strain two-fold bigger than type-II and type-III, that is why type-I crystals are characterized by higher values of work output (up to 12.8 $J \cdot cm^{-3}$) compared to types-I and type-III crystals (up to 5-6 $J \cdot cm^{-3}$). Work output values for NiTiHfPd obtained in this work exceed the same for $Ni_{49.5-x}Ti_{50.5}Pd_x$ (x = 15, 20, 25, 30, and 46 at. pct.) alloys (9 $J \cdot cm^{-3}$ at 300 MPa) [11] and for NiTiPd-20Hf alloys (4-5 $J \cdot cm^{-3}$ at 300 MPa) [3, 8].

Figure 3 also demonstrates the dependence of thermal hysteresis on stress level $\Delta T_\sigma(\sigma)$. Hysteresis is about the same 75-85 K for all studied states I-III at 250-300 MPa when maximal values of reversible strain are achieved. But at lower stress level the hysteresis value depends on the type of crystals. For example, the widest hysteresis 100 K is observed in type-I crystals under 50 MPa. After the heat treatments (type-II and type-III crystals) hysteresis values are 45 K and 70 K under 50 MPa, respectively.

In type-III crystals the hysteresis $\Delta T_\sigma(\sigma)$ almost doesn't depend on stress level and is equal to 75 K(±5 K) vs. type-I and type-II crystals, in which hysteresis values vary nonmonotonically with increase of stress level. Hysteresis values of type-I and type-II crystals increase up to 115 K and 75 K under 150 MPa, respectively.

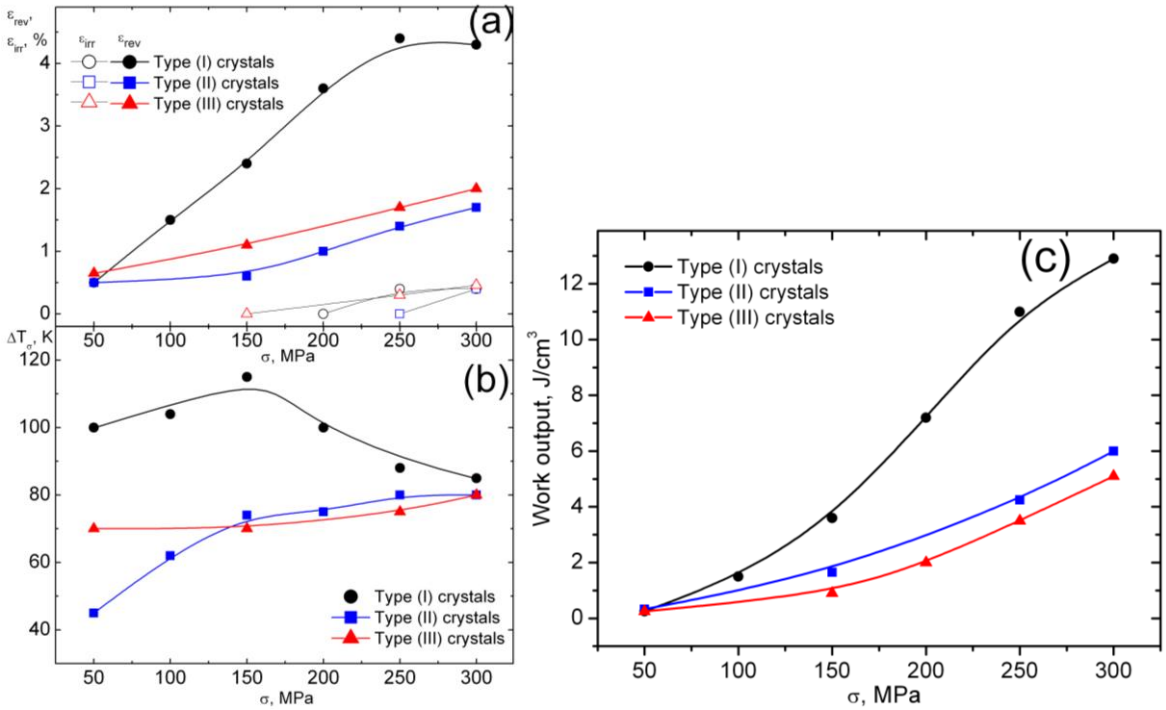

Figure 3. The dependences of reversible strain ε_{rev}, irreversible strain ε_{irr} (a), thermal hysteresis ΔT_σ (b) work output (c) on the applied stresses for type-I – type-III single crystals.

Then at σ>150 MPa, the decreasing of hysteresis is observed in type-I crystals, while hysteresis in type-II crystals doesn't change.

Figure 4 shows the σ(ε) response at loading/unloading in isothermal conditions. Given strain associated with stress-induced MT is reversible at unloading, so SE is observed. It is revealed that reversible strain values, obtained by ε(T) response, are close to values, obtained by σ(ε) response. The form of the σ(ε) curves depends on type of crystals. In type-I crystals the stress plateau with zero strain-hardening coefficient $\theta=d\sigma\cdot(d\varepsilon)^{-1}$ is observed. The θ value is raised up to $7.8\cdot10^4$ MPa with increase in stresses and so the transformation occurs with hardening. In type-III crystals there is no the plateau of stress and $\theta = 8.3\cdot10^4$ MPa.

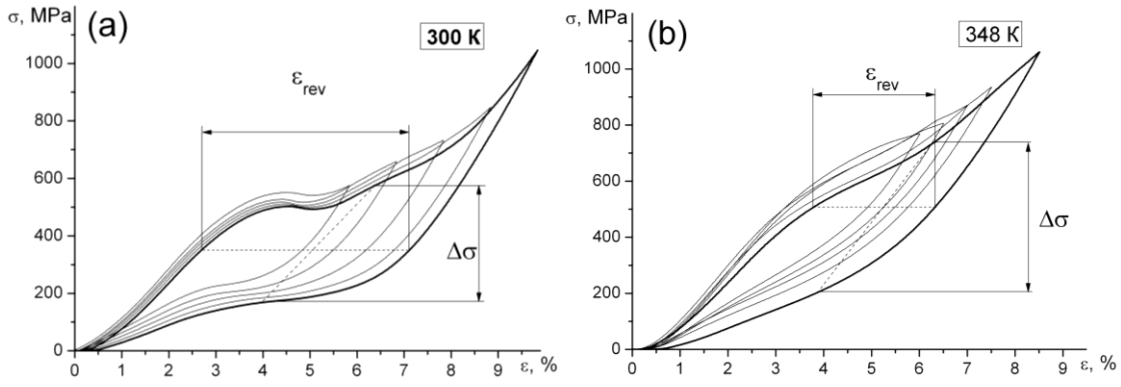

Figure 4. The σ(ε) response for type-I (a) and type-III (b) NiTiHfPd single crystals.

The stress hysteresis value increases with increase in given strain in type-I and type-III crystals. Also the reduction of critical stresses necessary for stress-induced MT is observed for type-I and type-III crystals by 36 MPa and 47 MPa, respectively. These are the evidence of formation of high amount

of defects during stress-induced MT. Mechanical hysteresis value at maximal reversible strain is about the same for type-I and type-III crystals and equal to 400 MPa and 460 MPa, respectively.

So, the energy dissipation characterized by stress and thermal hysteresis is similar in type-I and type-III crystals. Indeed the absorbed energy, evaluate as the area inside the hysteresis loop of σ(ε) response, is 17.3 $J \cdot cm^{-3}$ and 16.1 $J \cdot cm^{-3}$ for type-I and type-III crystals, respectively. These values are higher than obtained for aged $Ni_{45.3}Ti_{29.7}Hf_{20}Pd_5$ (at. %) single crystals [10], where the energy absorption capacity didn't exceed 8 $J \cdot cm^{-3}$.

Temperature dependence of critical stresses for stress-induced MT was obtained for all investigated crystals I-III as temperature dependence of critical stress $\sigma_{cr}(T)$ (by σ(ε) response) and dependence of temperature $M_{s'}$ on applied stress level (by ε(T) response). These dependences coincide and increase in stresses with the growth of temperature can be described by Clapeyron-Clausius equation (1):

$$\frac{d\sigma}{dT} = -\frac{\Delta S}{\varepsilon_{tr}} = -\frac{\Delta H}{T_0 \varepsilon_{tr}} \quad (1)$$

where ΔS – entropy of transformation, ΔH – enthalpy of transformation per unit volume, ε_0 – transformation strain, T_0 – temperature of chemical balance of martensite and austenite phases.

The coefficient $\alpha = d\sigma \cdot (dT)^{-1}$ characterizes the increase of stress level with the growth of temperature and depends on heat treatment: $\alpha_I = 3.4$ $MPa \cdot K^{-1}$, $\alpha_{II} = 5.3$ $MPa \cdot K^{-1}$, $\alpha_{III} = 5.4$ $MPa \cdot K^{-1}$. According to Clapeyron-Clausius equation the dependence of α on heat treatment is simply explained: the bigger value of α correspond to smaller value of transformation strain (figure 3, 5).

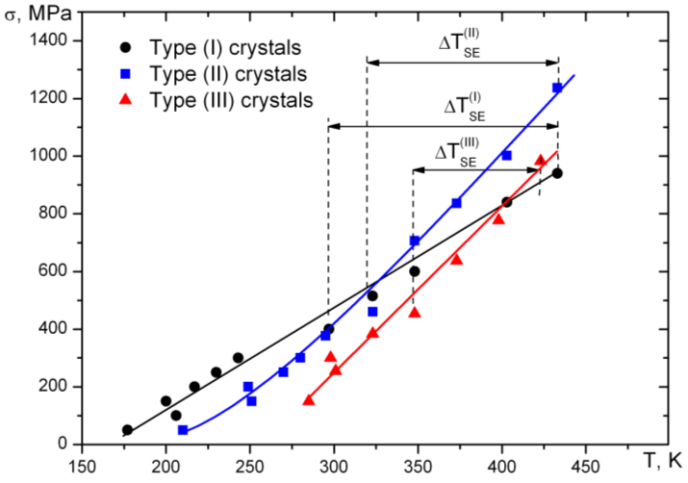

Figure 5. Temperature dependence of critical stress necessary for stress-induced MT in all investigated crystals I-III.

Figure 5 also shows the SE ranges. High-temperature SE (at T>373K) is observed in all investigated crystals and its temperature range depends on heat treatment. The widest SE range $\Delta T_{SE}(I) = T_{SE2} - T_{SE1} = 140$ K is observed in type-I crystals, whereas type-II and type-III crystals are characterized by a narrow SE ranges $\Delta T_{SE}(II) = 115$ K, $\Delta T_{SE}(III) = 75$ K. The temperature of the end of high-temperature SE range T_{SE2} is higher than temperature T_{SE2} for NiTiHfPd polycrystalline alloys [12] and NiTiPd-20Hf alloys [8], therefore, these single crystals can be used as high-temperature alloys with SE.

It is seen from figure 2 and figure 5, that thermal treatments provide the increase of MT temperatures. Increase of MT temperatures, coefficient θ and decrease of reversible strain after heat treatment can be associated with changes of the degree order of high-temperature phase and precipitation of the nano-size second-phase particles [13]. As follows from [3], particles of the second phase appear during aging at 500÷600 K [3]. Slow cooling after the homogenization could be the reason of precipitate of nano-size particle. Particles can provide the modification of chemical

composition of alloy, matrix strength, appearance of internal local stresses. Systematic TEM investigations are needed to clarify the reasons of such modification of features of stress-induced MT.

4. Summary

The effect of heat treatment on the features of stress-induced martensitic transformations was investigated in the [011]-oriented $Ni_{45.3}Ti_{29.7}Hf_{20}Pd_5$ (at. %) single crystals. It is experimentally shown, that the heat treatments $Ni_{45.3}Ti_{29.7}Hf_{20}Pd_5$ (at. %) single crystals that consist in homogenization at 1423 K for 4 h (type-II crystals) and followed by ageing at 1173 K for 3 h with water quenching (type-III crystals) result in following changes in comparison with as-grown single crystals: reversible strain reduces 2 times; $\alpha=d\sigma_{cr}\cdot(dT)^{-1}$ coefficient of critical stress growing is increased 1.5 times; the form or SE curves is changed: there isn't stress plateau and strain-hardening coefficient is increased.

Single crystals of $Ni_{45.3}Ti_{29.7}Hf_{20}Pd_5$ (at. %) alloys possess large temperature range of superelasticity (up to 140 K), large reversible strain (up to 4.3 %) and large value of absorbed energy and work output. These crystals can find the application as high-damping materials and solid-state actuator in the aerospace, automotive, and energy exploration industries at high temperatures.

Acknowledgments

This work was supported by Russian Science Foundation grant № 14-29-00012.

5. References

[1] Otsuka K and Wayman C M 1998 *Shape memory materials CUP* 284
[2] Acar E, Karaca H E, Basaran B, Yang F, Mills M J, Noebe R D and Chumlyakov Y I 2013 Role of aging time on the microstructure and shape memory properties of NiTiHfPd single crystals *Mater. Sci. Eng.* A **573** 161–5
[3] Acar E and Karaca H E 2014 Orientation dependence of the shape memory properties in aged $Ni_{45.3}Ti_{29.7}Hf_{20}Pd_5$ single crystals *Intermet.* **54** 60-8
[4] Frick C P, Ortega A M, Tyber J, Maksound A E M, Maier H J, Liu Y and Gall K 2005 *Mater. Sci. Eng.* A **405** 34–49
[5] Meng X L, Cai W, Chen F and Zhao L C 2006 *Scr. Metall.* **54** 1599–604
[6] Zarinejad M, Liu Y and Tong Y 2009 *Intermet.* **17** 914–9
[7] Stebner A P, Bigelow G S, Yang J, Shukla D P, Saghaian S M, Rogers R, Garg A, Karaca H E, Chumlyakov Y, Bhattacharya K and Noebe R D 2014 Transformation strains and temperatures of a nickel–titanium–hafnium high temperature shape memory alloy *Acta Mater.* **76** 40–53
[8] Acar E, Tobe H, Kaya I, Karaca H E and Chumlyakov Y I 2015 Compressive response of $Ni_{45.3}Ti_{34.7}Hf_{15}Pd_5$ and $Ni_{45.3}Ti_{29.7}Hf_{20}Pd_5$ shape-memory alloys *J. Mater. Sci.* **50** 1924-34
[9] Acar E, Karaca H E, Tobe H, Noebe R D and Chumlyakov Y I 2013 Characterization of the shape memory properties of a $Ni_{45.3}Ti_{39.7}Hf_{10}Pd_5$ Alloy *J. Alloys Compd.***578** 297–302
[10] Karaca H E, Acar E, Basaran B, Noebe R D, Bigelow G, Garg A, Yang F, Mills M J and Chumlyakov Y I 2012 Effects of aging on [111] oriented NiTiHfPd single crystals under compression *Scripta Mater* **67** 728–31
[11] Bigelow G S, Padula II S A, Garg A, Gaydosh D and Noebe R D 2010 Characterization of Ternary NiTiPd High-Temperature Shape-Memory Alloys under Load-Biased Thermal Cycling *Metall. Mater. Trans.* A **41A** 3065-79
[12] Karaca H E, Acar E, Ded G S, Basaran B, Tobe H, Noebe R D, Bigelow G and Chumlyakov Y I 2013 Shape memory behavior of high strength NiTiHfPd polycrystalline alloys *Acta Mater.* **61** 5036–49
[13] Hornbogen E, Mertinger V and Wurzel D 2001 Microstructure and tensile properties of two binary NiTi-alloys *Scripta Mater* **44** 171-8